

**HIGH-PRESSURE INFLUENCE ON PIRACETAM CRYSTALS: STUDYING  
BY QUANTUM CHEMICAL METHODS***Yuldasheva Nazokat Nikolayevna<sup>1</sup>*<sup>1</sup>*Khorezm Mamun branch of Uzbekistan Academy of Sciences**Ibragimov Aziz Bakhtiyarovich<sup>2</sup>*<sup>2</sup>*Director of the Institute of General and Inorganic  
Chemistry of the Academy of Sciences*

**Abstract.** In this study, we aim at developing a robust crystallization process for the ionic cocrystal between piracetam and  $\text{CaCl}_2$ . We discuss the structural characteristics of the piracetam- $\text{CaCl}_2$  cocrystal and its thermal behavior, furthermore we develop a robust crystallization process by construction of appropriate phase diagrams.  $\text{CaCl}_2$  and piracetam form an ionic dihydrate cocrystal with formula  $\text{piracetam} \cdot \text{CaCl}_2 \cdot \text{H}_2\text{O}$ , in which the  $\text{Ca}^{2+}$  cation adopts an octahedral coordination with the oxygens of 4 different molecules of piracetam and of two water molecules. According to the TGA, DSC and VT-XRPD, the cocrystal exhibits improved thermal stability compared to the parent drug compound. In this article we show how one can develop a robust, water-based cocrystallization process for ionic cocrystals, a relatively underexplored part of the cocrystal landscape. We also discuss the common ion effect on cocrystallization, and show how a common ion can strongly impact on the solubility of the cocrystal, as well as its constituting components. In addition, a common ion will also strongly impact the size of the cocrystal region in the ternary phase diagram.

**Keywords.** piracetam; hydrogen bond; crystal data; FT-IR spectroscopy; single crystal synthesis.

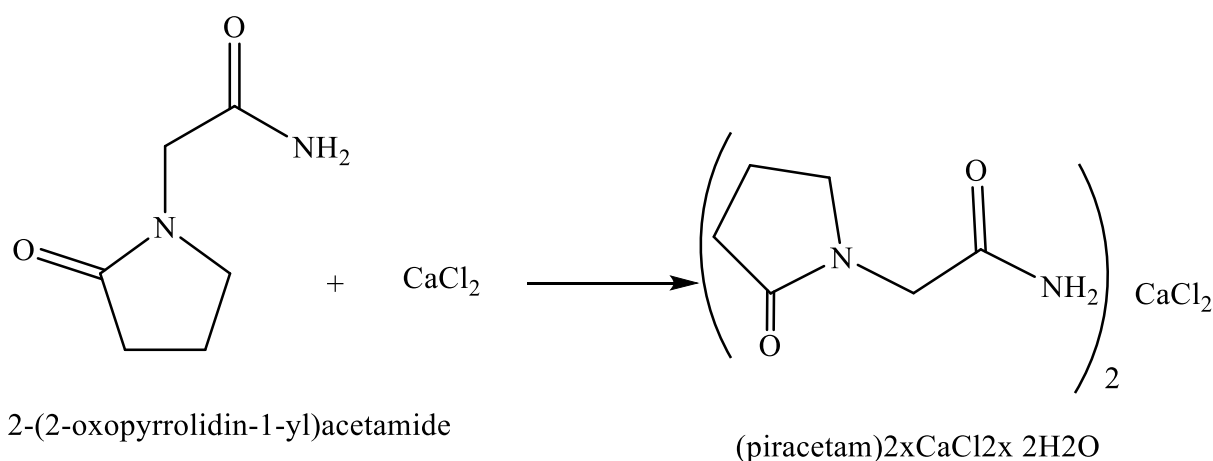
**Introduction.** Cocrystals, formed between an active pharmaceutical ingredient (API) and a cocrystal former, are garnering increasing interest within the pharmaceutical community as an appealing alternative for solid drug forms. By this time, scientists have achieved synthesize abundant type of uncommon cocrystals containing metal complex as a crystal former and auxiliary ligand[4-6]. These cocrystals offer enhancements to various pharmaceutically relevant properties compared to single-component crystals, including solubility, dissolution rate, hydration stability, fluorescence performance [1] and bioavailability. The interaction between the API and cocrystal former occurs via non-ionic and non-covalent intermolecular interactions, such as van der Waals forces and hydrogen bonding. Thus, the presence of unused hydrogen bond donor and acceptor sites is crucial for cocrystal formation [2, 3].

Salicylic acid finds application across various fields such as agriculture, cosmetics, and emerging pharmaceuticals due to its diverse biological properties. Its role as a crucial signaling molecule in regulating plant responses to environmental stress is widely recognized [5-6]. Literature survey reveals that numerous metal complexes formed with pharmacologically active ligands have demonstrated greater efficacy in treating diseases compared to the original ligands alone [7-8]. As a metal source we selected  $\text{Cu}^{++}$  salts to prepare metal complex. Recently, we reported the characterization of binuclear copper (II) salicylate complexes with DMFA, EtOH and water as second ligands [9-11]. Unlike them in the structure of the topic compound, unreacted piracetam crystallized via hydrogen bonds with salicylic acid carboxylic and hydroxyl group's oxygen.

Piracetam, also known as 2-oxo-pyrrolidineacetamide, is a nootropic drug that is widely utilized in the treatment of age-related cognitive decline and various nervous system disorders such as Alzheimer's disease and dementia [12]. With its dual amide moieties, piracetam provides an appropriate model pharmaceutical compound for exploring cocrystal formation. In this study, the investigation focuses on structural properties of the unusual cocrystal formed between piracetam and compound containing hydrogen bond acceptor groups, such as carboxylic acid or hydroxyl groups as example bi-nuclear copper tetrasalicylate[13-14].

### Experimental.

**Single Crystal Synthesis.** An equimolar mixture of Piracetam (14.2 mg, 1.00 mmol) and  $\text{CaCl}_2$  (11.1 mg, 1.00mmol) was dissolved in ethanol (2 ml) and left to evaporate over three days to get suitable crystals for single crystal,diffraction. Single crystals of  $\text{piracetam} \cdot \text{CaCl}_2 \cdot 2\text{H}_2\text{O}$  were obtained, as confirmed by single crystal x-ray diffraction and powder diffraction experiments Maintained in a constant temperature thermostat at  $40^\circ\text{C}$ , crystallization occurred over 25–27 days, yielding crystals with dimensions of  $1 \times 2 \times 1 \text{ mm}^3$  (Yield: 80%). (Scheme-1).



(Scheme-1). Synthesis of  $\text{piracetam} \cdot \text{CaCl}_2 \cdot 2\text{H}_2\text{O}$  salt.

### Single crystal X-ray structure analysis.

The crystal structure was elucidated by single-crystal XRD analysis. Crystallographic data and details of the refinement parameters are listed in Table-1. Single crystal X-ray diffraction was performed on a MAR345 image plate using monochromated MoK $\alpha$  radiation ( $\lambda = 0.71073$  Å) (Xenocs Fox3D mirror) produced by a Rigaku UltraX 18S rotating anode. The structures were solved by SHELXT and refined on  $|F_2|$  using SHELXL-2014/7. Non-hydrogen atoms were anisotropically refined and the hydrogen atoms in riding mode with isotropic temperature factors fixed at 1.2 times  $U(\text{eq})$  of the parent atoms.

Information of plane spacing for monoclinic structure crystal systems.

$$\frac{1}{d^2} = \frac{1}{\sin^2\beta} \cdot \left( \frac{h^2}{a^2} + \frac{k^2 \sin^2\beta}{b^2} + \frac{l^2}{c^2} - \frac{2hl \cos\beta}{ac} \right)$$

The selected hydrogen bonds, bond distances and bond angles are listed in Tables 2-4. The ORTEP and packing diagram of piracetam $\cdot$ CaCl $_2$   $\cdot$  2H $_2$ O are given in Fig-1. It crystallizes in the monoclinic system with centric space group Pn with Z = 2. The asymmetric unit consists of, electron density peak is found near heavy atom iodine. Crystal is a layered type that cannot be separated. This caused bad data quality and high  $wR_2$  value. Most of the amine/ammonium (R-NH $_2$ , R-NH $_3^+$ , etc.) containing crown ether complexes form N—H $\cdots$ O/N—H $\cdots$ O type of hydrogen bonds [5-9].

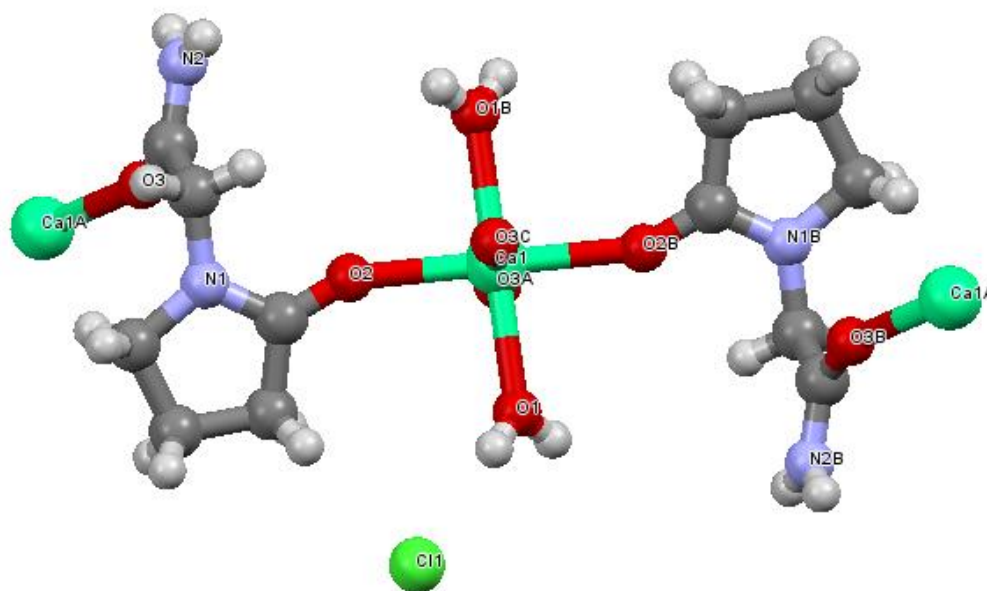


Fig-1. (a) ORTEP drawing of the intermolecular H-bonds and (b) piracetam $\cdot$ CaCl $_2$   $\cdot$  2H $_2$ O.

Thermal ellipsoids are drawn with the 50% probability level.

**Table -1. Crystal data and structure refinement for ) piracetam•CaCl<sub>2</sub> • 2H<sub>2</sub>O.**

Identification code	exp_393_CB08_auto
Empirical formula	C <sub>12</sub> H <sub>24</sub> CaN <sub>4</sub> O <sub>6</sub> 2(Cl)
Formula weight	431.33
Temperature/K	107(5)
Crystal system	Monoclinic
Space group	Pn
a/Å	12.70250(10)
b/Å	9.45940(10)
c/Å	19.25390(10)
α/°	90
β/°	92.3510(10)
γ/°	90
Volume/Å <sup>3</sup>	2311.56(3)
Z	2
ρ <sub>calc</sub> /g/cm <sup>3</sup>	1.487
μ/mm <sup>-1</sup>	11.216
F(000)	1060.0
Crystal size/mm <sup>3</sup>	0.14 × 0.12 × 0.11
Radiation	Cu Kα (λ = 1.54184)
2θ range for data collection/°	4.594 to 143.192
Index ranges	-15 ≤ h ≤ 15, -11 ≤ k ≤ 11, -23 ≤ l ≤ 23
Reflections collected	45306
Independent reflections	8957 [R <sub>int</sub> = 0.0551, R <sub>sigma</sub> = 0.0348]
Data/restraints/parameters	8957/2/520
Goodness-of-fit on F <sup>2</sup>	1.040
Final R indexes [I ≥ 2σ (I)]	R <sub>1</sub> = 0.0299, wR <sub>2</sub> = 0.0788
Final R indexes [all data]	R <sub>1</sub> = 0.0299, wR <sub>2</sub> = 0.0788
Largest diff. peak/hole / e Å <sup>-3</sup>	1.36/-1.55
Flack parameter	0.000

**Table-2. Hydrogen bonds for piracetam•CaCl<sub>2</sub> • 2H<sub>2</sub>O. (A<sup>0</sup>); R = 0.03.**

D-H...A	d(D-H)	d(H...A)	<DHA	d(D...A)	Symmetry
O1-H1...Cl1	0.8200	2.3500	2.866(6)	164.00	3/2-x,- 1/2+y,3/2-z
O1-H2...Cl1	0.8200	2.3400	2.994(5)	114.00	

N2–H11 •••C11	0.8600	2.5600	2.817(5)	149.00	
N2–H12 •••C11	0.8600	2.7900	2.918(5)	101.00	x,y,1+z
C5–H9 •••O2	0.9700	2.4600	2.876(6)	165.00	
C5–H9 •••C11	0.9700	2.4100	2.934(5)	117.00	1/2+x,3/2-y,1/2+z
C5–H10 •••C11	0.9700	1.9900	2.892(5)	174.00	1-x,2-y,1-z

**Table-3. Bond Distances [(P3MA)<sub>2</sub><sup>+</sup>·2(18C6)]·2H<sub>2</sub>O (A<sup>0</sup>). R = 0.03**

Bond	Distances	Bond	Distances
O(007)–C(00Q)	1.416(7)	O(00N)–H(G)	0.87(8)
O(007)–C(01G)	1.440(7)	O(00N)–H(00)	0.77(8)
O(00E)–C(014)	1.428(7)	N(00D)–C(016)	1.499(6)
O(00E)–C(015)	1.412(8)	N(00M)–C(01E)	1.340(7)
O(00G)–C(00Y)	1.429(7)	N(00M)–C(00J)	1.331(8)
O(005)–C(01D)	1.435(7)	C(00Q)–C(00S)	1.489(8)
O(005)–C(010)	1.438(7)	C(00Y)–C(018)	1.507(8)
O(006)–C(00W)	1.424(7)	C(012)–C(015)	1.501(8)
O(006)–C(00O)	1.403(7)	C(014)–C(01J)	1.489(9)
C(01J)–H(01R)	0.9900	C(01K)–H(3)	0.9500
C(010)–C(01C)	1.497(9)	C(00P)–C(00T)	1.503(7)

**Table-4. Bond Angles. (A<sup>0</sup>). R = 0.03**

Bond	Bond Angles	Bond	Bond Angles
C(00P)–N(00F)–H(00L)	109.00	H(00A)–C(00Q)–H(00B)	108.00
C(00P)–N(00F)–H(00M)	109.00	H(00C)–C(00S)–H(00D)	108.00
C(00Y)–C(018)–H(01G)	110.00	O(00A)–C(00X)–C(013)	108.9(5)
H(01I)–C(01A)–H(01J)	108.00	O(005)–C(010)–C(01C)	109.3(5)
O(00C)–C(013)–H(01X)	110.00	O(009)–C(01K)–H(3)	126.00
H(01W)–C(013)–H(01X)	108.00	N(00B)–C(00H)–C(00T)	123.5(4)
O(00I)–C(017)–H(B)	110.00	C(00T)–C(00L)–C(00V)	118.5(5)
N(00F)–C(00P)–C(00T)	112.9(4)	C(016)–C(00R)–C(01B)	121.3(5)
C(00H)–C(00T)–C(00P)	120.6(4)	C(016)–C(00R)–C(01E)	120.3(4)
C(00L)–C(00T)–C(00P)	121.1(4)	C(01B)–C(00R)–C(01E)	118.4(5)
C(00H)–C(00T)–C(00L)	118.2(4)	C(00J)–C(00Z)–C(01B)	118.2(5)
N(00B)–C(00U)–C(00V)	123.5(5)	N(00D)–C(016)–C(00R)	112.5(4)
C(00L)–C(00V)–C(00U)	119.3(5)	C(00R)–C(01B)–C(00Z)	118.9(5)
N(00B)–C(00H)–H(00N)	118.00	N(00M)–C(01E)–C(00R)	122.9(5)
C(00T)–C(00H)–H(00N)	118.00	C(00Z)–C(00J)–H(00X)	118.00

The percent elemental composition of compound 1,4,7,10,13,16-hexaoxacyclooctadecane, pyridin-3-ylmethanaminium salt was determined using a Thermo Scientific FlashSmart (CHNS/O) elemental analyzer. This analysis was performed by gas chromatographic separation of combustion gases based on the modified Dumas method. In order

to assess the accuracy of the measurements, the results obtained from the analysis were compared in practical and theoretical terms. Table-5

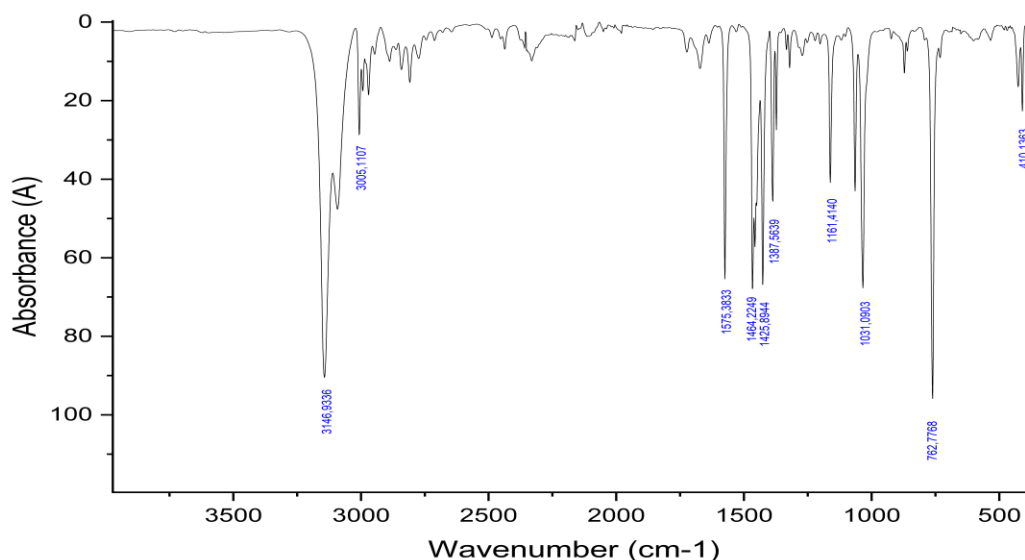
Table-5.

Compound	Mr	Compared	C %	H %	N %	O %
C <sub>12</sub> H <sub>24</sub> CaN <sub>4</sub> O <sub>6</sub> 2(Cl)	431.33 gr/mole	Theoretical	33.34	5.56	12.98	22.25
		Practical	33.18	5.49	12.78	21.96

**FT-IR spectroscopy.** The characteristics vibrational spectra of (I)-(V) are shown in Table-6.

To interpret the FT-IR spectrum of 1,4,7,10,13,16-hexaoxacyclooctadecane, pyridin-3-ylmethanaminium salt, we will assign each peak based on the structure and functional groups present in the compound. Below is a detailed analysis of the peaks you provided. Table-6.

Peak (cm <sup>-1</sup> )	Assignment	Functional group
3147	N-H stretching	-CH <sub>2</sub> -NH <sub>3</sub> <sup>+</sup> (protonated methanaminium group)
3005	Aromatic C-H stretching	Pyridine ring
1575	Aromatic C=C stretching or N-H bending	Pyridine ring or -CH <sub>2</sub> -NH <sub>3</sub> <sup>+</sup>
1464	Aromatic C-C stretching or N-H bending	Pyridine ring or -CH <sub>2</sub> -NH <sub>3</sub> <sup>+</sup>
1425	Aromatic ring deformation or C-H bending	Pyridine ring
1387	Symmetric C-H bending	-CH <sub>2</sub> - group
1161	Ether C-O stretching	Crown ether (-C-O-C-)
1031	Ether C-O stretching	Crown ether (-C-O-C-)
762	Out-of-plane C-H bending	Pyridine ring
410	Metal-ligand interaction or ring deformation	Crown ether or pyridine ring



### FT-IR spectroscopy- piracetam•CaCl<sub>2</sub>•H<sub>2</sub>O

**Conclusions.** In this contribution, we developed a robust, waterbased co-crystallization process for an ionic cocrystal, choosing piracetam-CaCl<sub>2</sub> as the model system. TGA, DSC and VT-XRD confirmed the dihydrated cocrystal Piracetam•CaCl<sub>2</sub>•2H<sub>2</sub>O to be stable up to 135 °C. Using water as a solvent a ternary phase diagram was developed showing a rather large congruent zone with the cocrystal as only stable phase in suspension. Based on this diagram, we developed an upscaled process for the manufacturing of Piracetam•CaCl<sub>2</sub>•2H<sub>2</sub>O. Finally, we illustrated the importance of the common ion effect on the crystallization of ICCs.

### REFERENCES.

1. Gouhie F. A. et al. Cognitive effects of piracetam in adults with memory impairment: A systematic review and meta-analysis // *Clinical Neurology and Neurosurgery*. – 2024. – C. 108358.
2. Mani V. et al. Piracetam as a therapeutic agent for doxorubicin-induced cognitive deficits by enhancing cholinergic functions and reducing neuronal inflammation, apoptosis, and oxidative stress in rats // *Pharmaceuticals*. – 2022. – T. 15. – №. 12. – C. 1563.
3. Abomosallam M. et al. Neuroprotective effect of piracetam-loaded magnetic chitosan nanoparticles against thiacloprid-induced neurotoxicity in albino rats // *Inflammopharmacology*. – 2023. – T. 31. – №. 2. – C. 943-965.
4. Attia K. A. M. et al. Environmentally sustainable DRS-FTIR probe assisted by chemometric tools for quality control analysis of cinnarizine and piracetam having diverged concentration ranges: Validation, greenness, and whiteness studies // *Spectrochimica Acta Part A: Molecular and Biomolecular Spectroscopy*. – 2023. – T. 302. – C. 123161.
5. Fan F. et al. Effect of organic acids on the solid-state polymorphic phase transformation of piracetam // *International Journal of Pharmaceutics*. – 2023. – T. 647. – C. 123532.

6. Liu J. et al. Piracetam reduces oxidative stress and mitochondrial function impairment in an in vitro model of vascular dementia // *Experimental Brain Research*. – 2024. – T. 242. – №. 8. – C. 1841-1850.

7. Wojszel Z. B. Nootropics (piracetam, pyritinol, co-dergocrine, meclophenoxat, pentoxifylline, nimodipine) // *NeuroPsychopharmacotherapy*. – Cham : Springer International Publishing, 2021. – C. 1-45.

8. Salamah A., Darwish A. H. Docosahexaenoic acid plus piracetam versus piracetam alone for treatment of breath-holding spells in children: a randomized clinical trial // *Pediatric Neurology*. – 2023. – T. 148. – C. 32-36.

9. Ihsan H. H. et al. Physicochemical investigations of nootropic drug piracetam for enhanced solubilization as nano drug carrier under the influence of single and mixed micellar formulations: An optimized approach towards drug delivery // *Journal of Molecular Liquids*. – 2024. – T. 407. – C. 125178.

10. Naik R. A. et al. Ameliorative effect of piracetam on emamectin benzoate induced perturbations in the activity of lactate dehydrogenase in murine system // *Advances in Redox Research*. – 2021. – T. 3. – C. 100019.

11. Mansour N. M. et al. Development of an Inexpensive, sensitive and green HPLC method for the simultaneous determination of brivaracetam, piracetam and carbamazepine; application to pharmaceuticals and human plasma // *Microchemical Journal*. – 2021. – T. 163. – C. 105863.

12. Liu T. et al. Efficacy and safety of compound porcine cerebroside and ganglioside injection (CPCGI) versus piracetam on cognition and functional outcomes for adults with traumatic brain injury: A study protocol for randomized controlled trial // *Heliyon*. – 2024. – T. 10. – №. 17.

13. Yuldasheva N. N. et al. Synthesis, structure, Hirshfeld surface analysis, and molecular docking studies of the cocrystal between the Cu (II) complex of salicylic acid and uncoordinated piracetam // *Turkish Journal of Chemistry*. – 2024. – T. 48. – №. 6. – C. 809-820.

14. Borozdenko D. A. et al. A novel phenylpyrrolidine derivative: synthesis and effect on cognitive functions in rats with experimental ischemic stroke // *Molecules*. – 2021. – T. 26. – №. 20. – C. 6124.

15. El-Dessouki A. M. et al. Piracetam mitigates nephrotoxicity induced by cisplatin via the AMPK-mediated PI3K/Akt and MAPK/JNK/ERK signaling pathways // *International Immunopharmacology*. – 2024. – T. 137. – C. 112511.

16. Pottoo F. H. et al. Therapeutic enhancing potential of piracetam with diethylstilbestrol in prevention of grand-mal seizures in rats: inhibition of PI3K/Akt/mTOR signaling pathway and IL-1 $\beta$ , IL-6, TNF- $\alpha$  cytokines levels // *European Review for Medical & Pharmacological Sciences*. – 2023. – T. 27. – №. 10.